CATECHOL DETETION USING AN OPTICAL MEMS SENSOR

Peter H. Dykstra, Stephan T. Koev, Reza Ghodssi
MEMS Sensors and Actuators Lab, Department of Electrical and Computer Engineering
Institute for Systems Research (ISR), University of Maryland, College Park, MD 20742, U.S.A.

Gregory F. Payne
University of Maryland Biotechnology Institute (UMBI), Rockville, MD 20850, U.S.A.

Liangli Yu
Department of Nutrition and Food Science, University of Maryland, College Park, MD 20742, U.S.A.

Keywords: Catechol, Chitosan, Waveguides, Absorbance.

Abstract: We report the successful fabrication and testing of an optical MEMS sensor for the detection of the toxic phenol, catechol. Catechol's presence in food and drinking water posses a health concern due to its harmful effects on cell respiration. By-products of catechol oxidation have demonstrated increased absorbance changes in a chitosan film in the UV and near UV range. Our reported sensor takes advantage of this unique absorbance property to detect catechol by measuring the change in light intensity at 472 nm, thus eliminating non-specific responses that occur from other oxidized chemicals which do not cause the absorbance change. Concentrations as low as 1 mM catechol are detected while control experiments including ascorbic acid display no measurable response.

1 INTRODUCTION

Monitoring the safety of our water supply by using portable, efficient and inexpensive devices has become an area of growing interest over the past decade. The growth of industry has contributed to the contamination of ground waters with various potentially dangerous organic chemicals. Catechol is a synthetic phenol commonly generated in factory processes and it has been proven to have detrimental health effects (Starek, 2003). One monitoring solution is through the use of microelectromechanical systems (MEMS) to create on-chip sensors which can give field personnel accurate and sensitive data on-site regarding the testing of the water supply.

Recently reported sensors for catechol detection either use optical or electrochemical measurement schemes. Optical sensors making use of absorbance (Abdullah et al., 2006) and fluorescence (Wu et al., 2004) detection have been reported but the necessity for bulky, external measuring equipment has hindered the fabrication of such devices on chip. Electrochemical sensors typically employ a standard three electrode system with the working electrode covered by an immobilization matrix such as calcium carbonate to entrap oxidizing enzymes (Shan et al., 2007). Although these devices result in high sensitivity, the enzyme activity degrades over time and can be directly affected by certain conditions such as the pH of the solution making these sensors difficult to calibrate.

Our reported device utilizes an optical absorbance technique in a sealed microfluidic channel for the detection of catechol. In order to amplify the effect of the detected absorbance by catechol oxidation, the aminopolysaccharide chitosan is deposited in the microfluidic channel, thus intersecting the pathway of the light through the device. The proposed detection scheme does not require the use of enzymes yet still remains selective to phenolic compounds vs other chemical agents.

Dykstra P., Koev S., Ghodssi R., Payne G. and Yu L. (2009).
CATECHOL DETETION USING AN OPTICAL MEMS SENSOR.
In *Proceedings of the International Conference on Biomedical Electronics and Devices*, pages 104-108
DOI: 10.5220/0001552001040108

2 MATERIALS AND THEORY

2.1 Catechol

Catechol is a benzenediol, which is a subset of the phenol class of organic compounds. The chemical formula of Catechol is $C_6H_4(OH)_2$. Following oxidation, catechol loses its hydrogen atoms from the hydroxyl groups and becomes an orthobenzoquinone, more commonly referred to as an *o*-quinone. The oxidation of catechol in the cell creates free radicals which cause damage to vital cell components such as lipids, proteins and DNA (Sies, 1997).

2.2 Chitosan

Chitosan is a unique material that is well suited for biological micro-devices due to its ability to be selectivity deposited and its high density of amine groups, which provide active bonding sites. The selective deposition occurs due to chitosan's insolubility above a pH of 6.5. At low pH, chitosan is protonated and soluble in water. As the pH rises above 6.5, the amines lose their net positive charge and the chitosan becomes insoluble. By taking advantage of this property, one can deposit a film of chitosan onto a cathode during an electrochemical reaction. The pH rises with increasing proximity to the cathode due to the reduction of the hydrogen ions. The chitosan forms as a thin film or hydrogel over the cathode surface depending on the amplitude of the applied current density.

Chitosan has an added advantage over other polysaccharides because it contains nucleophilic primary amine (NH_2) groups at nearly every repeating sugar residue in its structure. The *o*-quinones, which are formed from the oxidized catechol molecules, bind to the amine groups and impart physical changes to the film, such as a change in the optical absorbance (Wu et al., 2005).

2.3 Optics

Understanding the operating principle of the device requires a more detailed understanding of light propagation and absorption through a medium. The absorbance can be related to the concentration of absorbing species present as demonstrated by the Beer-Lambert Law:

$$A = -\log_{10}\left(\frac{I_1}{I_0}\right) = \varepsilon l c \qquad (1)$$

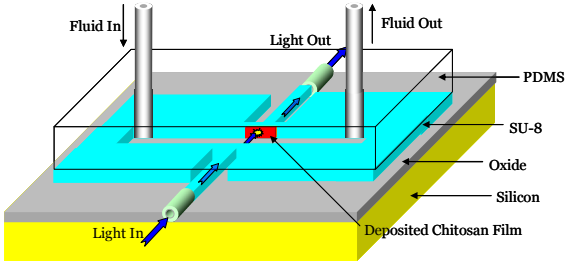

Figure 1: 3-d Schematic of the packaged device. The device dimensions are 3.2 x 2.4 x 0.24 cm.

Where ε is the molar absorptivity, l is the path length the light takes as it propagates through the absorbing layer and c is the concentration. In our experiments, the path length, l, is defined as the thickness of the deposited chitosan film. *O*-quinones have been reported to show a strong absorbance in the UV and near UV range of the electromagnetic spectrum (Wu et al., 2005). For this reason, a blue laser source at 472 nm was chosen for the optical measurements taken with the MEMS sensor.

In our device, on-chip waveguides are patterned from the polymer SU-8 as shown in the device schematic (Figure 1). Blue light is coupled in and out of the waveguides via multimode fibers with a core diameter of 62.5 µm. The cross sectional area of the polymer waveguides is 100 µm by 150 µm. The light propagates through a film of chitosan that has been deposited onto a transparent, conductive film of indium tin oxide.

Since the absorbance measurement is purely related to the optical power being received, it is important to understand the different optical loss mechanisms through the device in order to achieve an acceptable signal to noise ratio. The primary sources of loss are caused by waveguide losses which include material absorption and scattering, divergence of the light crossing the channel, and roughness associated with the waveguide facets.

Waveguide loss will occur due to the roughness of the waveguide and any material absorption through the SU-8. This attenuation was measured to be 21.15 dB/cm at 472 nm for waveguides with our dimensions using image processing software. A top-down digital photograph was taken of fabricated test waveguides coupled to a blue laser source. The light intensity down the length of the waveguide was analyzed to determine the attenuation coefficient.

Divergence of the light as it crosses the microfluidic channel from one waveguide to the next is another possible source of loss. The light capturing efficiency from one waveguide to the next is found by integrating the surface energy of a beam

with a Gaussian profile and is related to the width of the beam waist as seen in (2).

$$\eta = \frac{2w(z) * w_0}{w(z)^2 + {w_0}^2} \quad (2)$$

Where w_0 and w(z) are the width of the beam waist before and after it has traversed the channel. For the dimensions used in our device, the coupling efficiency of the light as it traverses the channel from one waveguide to another is near unity (η = 0.99). The high coupling efficiency is a result of using waveguides with large cross sectional areas. With these considerations, the most significant factor that contributes to optical loss in the device is the roughness of the waveguide facets and sides. The surface roughness of the waveguides is an inherent limitation when using lithography and cannot be completely avoided.

3 DEVICE FABRICATION

3.1 Wafer Level Processes

The MEMS sensor was fabricated using conventional MEMS patterning techniques. Four inch silicon wafers (<100> orientation) begin with a one µm thick thermal SiO_2 to act as a bottom cladding layer for the waveguides. Layers of chrome (20 nm) and gold (200 nm) are sputtered onto the oxide coated wafers and patterned to create the electrodes inside the microfluidic channels.

SU-8 was applied to the wafer and spun first at 600 RPM for 10 seconds followed by 1150 RPM for 30 seconds to achieve a final thickness of 100 µm. The pre-bake was performed on a hotplate at 55°C for 2 hours with a temperature ramp of 5 degrees per minute.

The SU-8 was exposed to UV light at a dose of 2500 mJ/cm^2 using a mask aligner system, and then placed back on the hotplate to bake at 55°C for 90 minutes with a temperature ramp of 5 degrees per minute. After post-baking, the SU-8 was developed for 10 minutes.

A film 200 nm thick of indium tin oxide (ITO) was deposited on the wafer using RF magnetron sputtering. The sidewall patterning procedure of the ITO using AZ9245 photoresist has been described elsewhere (Powers et al., 2005). The wafers are cleaned using acetone, methanol, isopropyl alcohol and DI water, then diced into individual dies for testing.

3.2 Die-level Processes

Medium molecular weight (~200 kDa) chitosan flakes were purchased from Sigma Aldrich and prepared using established methods resulting in a solution with pH of 5.3 and w/v chitosan of 0.5% (Yi et al., 2005). The chitosan solution was applied to the active electrode area using a 100 µl syringe and biased at a current of 0.35 µA, which corresponds to a current density of 4 A/m^2. This procedure results in complete chitosan coverage of the sidewall interface. The current was applied for 10 minutes, after which the device was rinsed extensively with DI water and blown dry with nitrogen.

The deposited chitosan films were measured to be between 5 and 10 microns thick by measuring the distance the chitosan extends from the sidewall using an optical microscope. Following deposition and rinsing, the chips are immersed in a 1 M solution of NaOH for 5 minutes to neutralize the chitosan film.

The fluidic channel was sealed using a thick (1 mm) flexible polymer, PDMS. PDMS curing agent and polymer were purchased from Sigma Aldrich and mixed in a 1:10 ratio. The solution was cured at 80°C for 25 minutes in a box furnace, and then cut into smaller pieces to fit over the device. To position the PDMS layer, methanol is applied to one side and the PDMS is slid into place over the device.

Metal capillaries with OD 400 µm and ID 200 µm were inserted through the PDMS to create liquid inlet and outlet ports. Multimode optical fibers were aligned to the on-chip waveguides through the use of patterned grooves in the SU-8 resist. Once aligned by hand under a stereomicroscope, an adhesive was used to secure the fiber. The final packaged device is shown in figure 2.

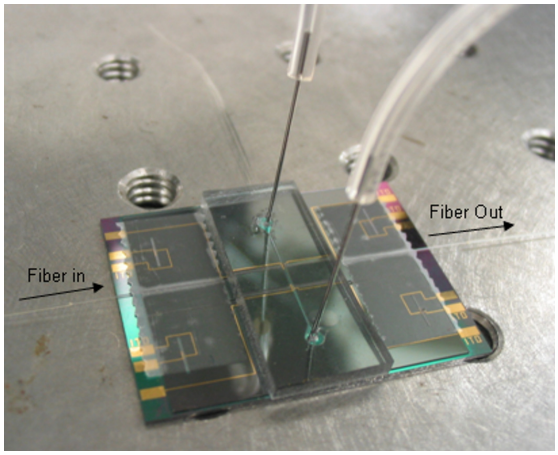

Figure 2: Photograph of packaged device.

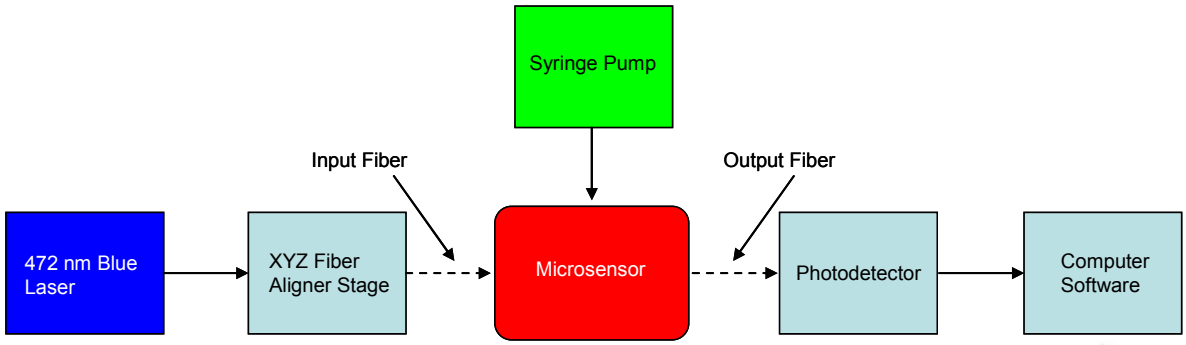

Figure 3: Block Diagram of testing setup for the MEMS sensor.

4 TESTING AND RESULTS

Absorbance measurements from catechol oxidation were taken using blue light (472 nm) coupled through the MEMS device. Figure 3 displays a graphic of the testing setup used. Light was delivered from a free space blue laser (LaserMate, Pomona, CA) operating in the continuous wave mode and focused into a multimode fiber using a manual alignment stage. Output light was coupled via the optical fiber to a USB linked spectrophotometer (Ocean Optics, Dunedin, FL) which facilitated automated data collection using software. Catechol flakes were purchased from Sigma Aldrich and dissolved in a 20 mM phosphate buffer at a pH of 5.3. Liquid was administered using a GENIE PLUS syringe pump (Kent Scientific, Torrington, CT) at a flow rate of 100 µl/hr, which translates to a linear flow velocity in the channel of about 1 mm/s. All of the experiments were performed at room temperature.

Figure 4 displays the change in measured light intensity for three different catechol concentrations after they were oxidized for 10 minutes at a current density of 4A/m^2. No decrease in intensity was observed from the oxidation of the buffer solution or the common antioxidant, ascorbic acid. Also shown are measurements for devices without the chitosan film. The data clearly demonstrates the necessity of the chitosan in order to detect smaller concentrations of catechol. Devices with the chitosan film display a 3x and 7x signal increase vs. those without chitosan for 100 mM and 10 mM catechol concentrations respectively. At our lowest measured concentration of 1 mM, no change in the light intensity is detected for the device without the chitosan film. The chitosan film amplifies the signal because it effectively traps the generated *o*-quinones at the sensing area of the device through covalent bonding. It should be noted that these tests without chitosan require the liquid flow to be stopped in the channel. Any applied flow rate will cause the *o*-quinones to be swept away from the sensing area, disallowing any accumulation which would cause a detectable change in absorbance. Measurement error was calculated based on the observed fluctuations in the intensity measurement due to either changes in the laser power or noise effects in the detector.

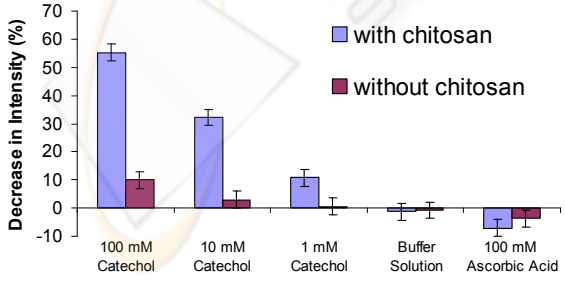

Figure 4: Measured decrease in light intensity at 472 nm after 10 minute oxidation at 4 A/m^2. A clear signal increase is displayed for all catechol concentrations when using chitosan in the device.

The increasing absorbance change over the 10 minute period for each sample is displayed in figure 5. The accumulation of the *o*-quinones is roughly the same for each concentration of catechol for the first minute as the rate is primarily reaction limited. Over

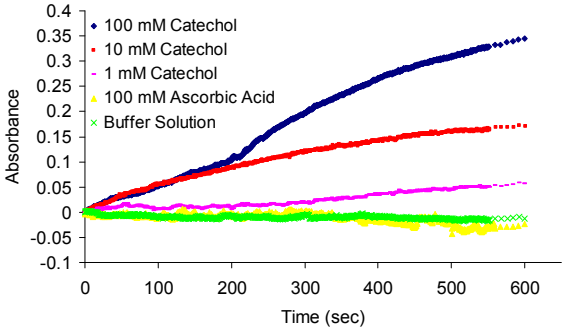

Figure 5: Change in absorbance over time for each sample.

time, the absorbance rate becomes diffusion limited as the catechol must traverse through the chitosan film to reach the electrode.

5 CONCLUSIONS

We report the demonstration of on-chip catechol detection using optical absorbance measurements. The device successfully demonstrates selective detection of phenolic (catechol) vs. non-phenolic (ascorbic acid) compounds without the need of enzymes. The device also exhibits good differentiation for a wide range of catechol concentrations. Since our device uniquely allows for the collection of time resolved absorbance data, calibration curves can be fit to different times in order to achieve more accurate sensing of the concentration. The analysis performed in this research can hopefully help to provide the groundwork for a device used for the detection of catechol packaged in a low-cost, portable system.

ACKNOWLEDGEMENTS

The authors would like to thank the National Science Foundation (NSF-EFRI) and the R. W. Deutsch Foundation for funding this research.

REFERENCES

Abdullah, J., Ahmad, M., Karuppiah, N., Heng, L. Y. & Sidek, H. (2006) Immobilization of tyrosinase in chitosan film for an optical detection of phenol. *Sensors and Actuators B,* 114**,** 604-609.

Powers, M. A., Koev, S. T., Schleunitz, A., Yi, H., Hodzic, V., Bentley, W. E., Payne, G. F., Rubloff, G. W. & Ghodssi, R. (2005) A fabrication platform for electrically mediated optically active biofunctionalized sites in BioMEMS. *Lab on a Chip,* 5**,** 583-586.

Shan, D., Zhu, M., Han, E., Xue, H. & Cosnier, S. (2007) Calcium carbonate nanoparticles: A host matrix for the construction of highly sensitive amperometric phenol biosensor. *Biosensors and Bioelectronics,* 23**,** 648-654.

Sies, H. (1997) Oxidative stress: oxidants and antioxidants. *Experimental Physiology,* 82**,** 291-295.

Starek, A. (2003) Estrogens and Organochlorine Xenoestrogens and Breast Cancer Risk. *International Journal of Occupational Medicine and Environmental Health,* 16**,** 113-124.

Wu, L.-Q., Ghodssi, R., Elabd, Y. A. & Payne, G. F. (2005) Biomimetic Pattern Transfer. *Advanced Functional Materials,* 15**,** 189-195.

Wu, X. J., Choi, M. M. F. & Wu, X. M. (2004) An organic-phase optical phenol biosensor coupling enzymatic oxidation with chemical reduction. *The Analyst,* 129**,** 1143-1149.

Yi, H., Wu, L.-Q., Bentley, W. E., Ghodssi, R., Rubloff, G. W., Culver, J. N. & Payne, G. F. (2005) Biofabrication with chitosan. *Biomacromolecules,* 6**,** 2881-2894.